A Critical Role for Dna2 at Unwound Telomeres

Marta Markiewicz-Potoczny,* Michael Lisby,† and David Lydall*,1

*Institute for Cell and Molecular Biosciences, The Medical School, Newcastle University, Newcastle upon Tyne NE2 4HH, United Kingdom and †Department of Biology, University of Copenhagen, DK-2200, Denmark

ORCID IDs: 0000-0002-3586-6977 (M.M.-P.); 0000-0002-4830-5247 (M.L.); 0000-0003-2478-085X (D.L.)

ABSTRACT Dna2 is a nuclease and helicase that functions redundantly with other proteins in Okazaki fragment processing, double-strand break resection, and checkpoint kinase activation. Dna2 is an essential enzyme, required for yeast and mammalian cell viability. Here, we report that numerous mutations affecting the DNA damage checkpoint suppress *dna2*Δ lethality in *Saccharomyces cerevisiae*. *dna2*Δ cells are also suppressed by deletion of helicases *PIF1* and *MPH1*, and by deletion of *POL32*, a subunit of DNA polymerase δ. All *dna2*Δ cells are temperature sensitive, have telomere length defects, and low levels of telomeric 3′ single-stranded DNA (ssDNA). Interestingly, Rfa1, a subunit of the major ssDNA binding protein RPA, and the telomere-specific ssDNA binding protein Cdc13, often colocalize in *dna2*Δ cells. This suggests that telomeric defects often occur in *dna2*Δ cells. There are several plausible explanations for why the most critical function of Dna2 is at telomeres. Telomeres modulate the DNA damage response at chromosome ends, inhibiting resection, ligation, and cell-cycle arrest. We suggest that Dna2 nuclease activity contributes to modulating the DNA damage response at telomeres by removing telomeric C-rich ssDNA and thus preventing checkpoint activation.

KEYWORDS Dna2; telomere; yeast

THE conserved nuclease/helicase Dna2 affects 5′ processing of Okazaki fragments during lagging strand replication (Budd and Campbell 1997), resection of double-strand breaks (DSBs)/uncapped telomeres (Ngo *et al.* 2014), activation of DNA damage checkpoint pathways (Kumar and Burgers 2013), resolution of G quadruplexes (Lin *et al.* 2013), and mitochondrial function (Budd *et al.* 2006; Duxin *et al.* 2009). Increased expression of *DNA2* is found in a broad spectrum of cancers, including leukemia, melanoma, breast, ovarian, prostate, pancreatic, and colon cancers (Peng *et al.* 2012; Dominguez-Valentin *et al.* 2013; Strauss *et al.* 2014; Jia *et al.* 2017; Kumar *et al.* 2017; Wellcome Sanger Institute). Dna2 is an important enzyme because its loss is lethal in human cell lines, mice, *Caenorhabditis elegans*, budding yeast, and fission yeast (Budd *et al.*

1995; Kang *et al.* 2000; Lin *et al.* 2013). The amount of Dna2 in cells also seems to be important as *dna2*Δ*/DNA2* heterozygous mice show increased levels of aneuploidy-associated cancers and cells from these mice contain high numbers of anaphase bridges and dysfunctional telomeres (Lin *et al.* 2013).

In budding yeast Dna2 functions redundantly with other proteins in its various roles and intriguingly, unlike Dna2, most of these proteins are not essential. For example, Rad27, Rnh201, and Exo1 are all nonessential and are also involved in processing of 5′ ends of Okazaki fragments (Bae *et al.* 2001; Kao and Bambara 2003). Exo1, Sgs1, Sae2, Mre11, Rad50, and Xrs2 are all nonessential and are involved in DSB resection (Mimitou and Symington 2008; Zhu *et al.* 2008; Shim *et al.* 2010). Ddc1 (nonessential) and Dpb11 (essential) are involved in Mec1 (essential) checkpoint kinase activation (Puddu *et al.* 2008; Navadgi-Patil and Burgers 2009a,b; Kumar and Burgers 2013). Given that Dna2 often functions redundantly with nonessential proteins, it is unclear what specific function or functions of Dna2 is/are so critical for cell viability.

Several genetic and biochemical experiments have suggested that the most critical function of Dna2 is in processing long flaps at a small subset of 5′ ends of Okazaki fragments (Budd *et al.* 2011; Balakrishnan and Bambara 2013). Dna2 is unique in that, unlike the other 5′ nucleases (Rad27, Exo1, Rnh201), it can cleave RPA-coated single-stranded DNA (ssDNA) (Stewart *et al.*

2008; Cejka *et al.* 2010; Levikova *et al.* 2013; Levikova and Cejka 2015; Myler *et al.* 2016). RPA, the major eukaryotic ssDNA binding protein, binds ssDNA of 20 bases or more (Sugiyama *et al.* 1997; Rossi and Bambara 2006; Balakrishnan and Bambara 2013). Furthermore, RPA-coated ssDNA is potentially lethal because it stimulates DNA damage checkpoint responses (Lee *et al.* 1998; Zou and Elledge 2003).

Two reported null suppressors of *dna2*Δ lethality, *rad9*Δ and *pif1*Δ, delete proteins that interact with RPA-coated ssDNA (Budd *et al.* 2006, 2011). Rad9 is important for the checkpoint pathway stimulated by RPA-coated ssDNA (Lydall and Weinert 1995). Pif1, a 5′ to 3′ helicase, increases the length of 5′ ssDNA flaps on Okazaki fragments, creating substrates for RPA binding and therefore checkpoint activation and Dna2 cleavage (Pike *et al.* 2009; Levikova and Cejka 2015). These genetic and biochemical data supported a model in which Dna2 is critical for cleaving RPA-coated long flaps from a subset of Okazaki fragments (Budd *et al.* 2011). However, more recently it was reported that other checkpoint mutations (*ddc1*Δ or *mec1*Δ) also affecting the response to RPA-coated ssDNA did not suppress *dna2*Δ (Kumar and Burgers 2013). It was suggested that specific interactions between Rad9 and Dna2 were important for the viability of *dna2*Δ *rad9*Δ cells, rather than the response to RPA-coated ssDNA *per se* (Kumar and Burgers 2013).

In budding yeast, checkpoint mutations such as *rad9*Δ and *ddc1*Δ exacerbate fitness defects caused by general DNA replication defects (*e.g.*, defects in DNA ligase, Pol α, Pol ε, or Pol δ) (Weinert *et al.* 1994; Dubarry *et al.* 2015), but suppress defects caused by mutations affecting telomere function (*e.g.*, defects in Cdc13, Stn1, Yku70) (Addinall *et al.* 2008; Holstein *et al.* 2017). The opposing effects of checkpoint mutations in general DNA replication or telomere-defective contexts is most likely explained by damage to noncoding telomeric DNA being comparatively benign in comparison to damage to coding DNA in the middle of chromosomes. By this logic, the suppression of *dna2*Δ by *rad9*Δ implies that *dna2*Δ might cause telomere-specific rather than general chromosome replication defects. Furthermore, Dna2 localizes to human and yeast telomeres (Choe *et al.* 2002; Chai *et al.* 2013; Lin *et al.* 2013), and *pif1*Δ, which suppresses *dna2*Δ, affects a helicase that is active at telomeres and affects telomere length (Dewar and Lydall 2010; Budd and Campbell 2013; Lin *et al.* 2013; Phillips *et al.* 2015). Thus, several lines of evidence suggest that Dna2 might play critical function(s) at telomeres.

To further explore whether Dna2 is important at telomeres, we set out to clarify the effects of checkpoint pathways on fitness of *dna2*Δ mutants. We find that deletion of numerous DNA damage checkpoint mutations, all affecting responses to RPA-coated ssDNA, as well as deletions of Pif1 and Mph1 helicases, and Pol32, a subunit of Pol δ, suppress *dna2*Δ to a similar extent. These findings, along with a number of other telomere phenotypes lead us to suggest that the most critical function of Dna2 for cell viability is at telomeres. There are three possible substrates for Dna2 activity at telomeres: unwound telomeres, long flaps on terminal telomeric Okazaki fragments, and G4 quadruplexes formed on the G-rich ssDNA. We propose that the critical function of Dna2 is removing RPA-coated, 5′ C-rich, ssDNA at telomeres.

Materials and Methods

Yeast culture and passage

All yeast strains were in W303 background and *RAD5+* and *ade2-1*, except strains used for microscopy, which were *ADE2*. Strains and plasmids details are in Supplemental Material, Tables S1 and S2 in File S1, respectively. Strains and plasmids are available upon request. Media were prepared as described previously and standard genetic techniques were used to manipulate yeast strains (Sherman *et al.* 1986). YEPD (1 liter: 10 g yeast extract, 20 g bactopeptone, 50 ml 40% dextrose, 15 ml 0.5% adenine, 935 ml H_2O) medium was generally used. Dissected spores were germinated for 10–11 days at 20°, 7 days at 23°, or 3–4 days at 30°. Colonies from spores on germination plates were initially, instead of patched onto YEPD medium plates and grown for 3 days. Next. these were streaked for single colonies and incubated for 3 days at 23°. Thereafter, 5–10 colonies of each strain were pooled by toothpick and streaked for single colonies every 3 days.

Yeast spot test assays

A total of 5–10 colonies were pooled, inoculated into 2 ml YEPD medium and grown to saturation on a wheel at 23°. Saturated cultures were fivefold serially diluted in sterile water (40:160 µl) in 96-well plates. Cultures were transferred onto rectangular YEPD medium agar plates with a rectangular pin tool, and incubated at the indicated temperatures for 3 days before photography, unless stated otherwise.

In-gel assay/Southern blots

In-gel assays were performed as previously described (Dewar and Lydall 2012), with minor modifications. Infrared 5′ IRDye 800 probes were used (AC probe: M3157, *CCCACCACACACA CCCACACCC*; TG probe: M4462, *GGGTGTGGGTGTGTGT GGTGGG*; Integrated DNA Technologies). No RNAse was used during nucleic acid purification. Samples were run on a 1% agarose gel in 0.5× TBE (50 V for 3 hr), and the probe was detected on a LI-COR (Odyssey) imaging system. ssDNA was quantified using ImageJ. The gel was then placed back in an electrophoresis tank, run for 2 hours, and processed for Southern blotting. Then, gel was stained using SYBR Safe, and DNA was detected using a Syngene's G:BOX imaging system. DNA was then transferred to a positively charged nylon membrane. The membrane was hybridized with a 1 kbp Y′ and TG probe, as previously described (Holstein *et al.* 2014). Loading controls were generated by foreshortening the full-sized SYBR Safe-stained gel images with Adobe Illustrator CS6.

Yeast live-cell imaging

Cells were grown shaking in liquid synthetic complete medium supplemented with 100 µg/ml adenine at 25°, to OD_{600} = 0.2–0.3, and processed for fluorescence microscopy as described previously (Silva *et al.* 2012). Rfa1 was tagged with
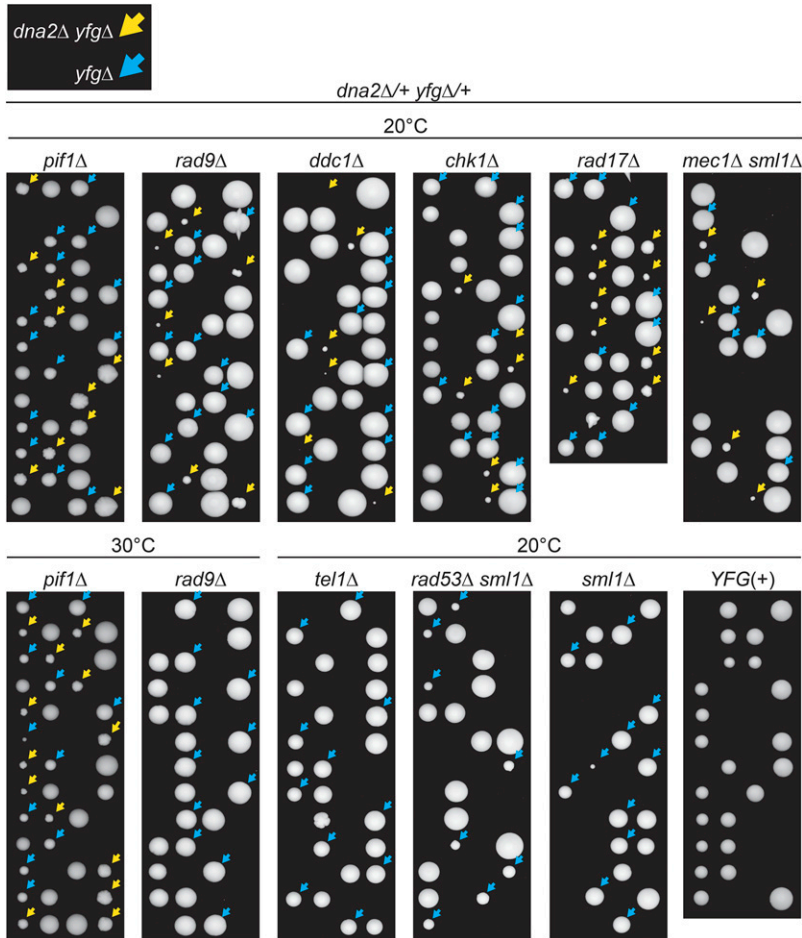
Figure 1 Checkpoint mutations permit growth of *dna2Δ* cells at 20°. Diploids heterozygous for *dna2Δ* and *pif1Δ*, *rad9Δ*, *ddc1Δ*, *chk1Δ*, *rad17Δ*, *mec1Δ sml1Δ*, *tel1Δ*, *rad53Δ sml1Δ* or *sml1Δ* mutations were sporulated, tetrads were dissected, and spores germinated. Germination plates were incubated for 10–11 days at 20°, or 3–4 days at 30°. Strains of *dna2Δ yfgΔ* background are indicated by yellow arrows, and strains of *yfgΔ* background are indicated by blue arrows. Additional images of growth at 20, 23, or 30° are in Figure S1 in File S1. Strains were as follows: DDY1285, DDY874, DDY876, DDY878, DDY880, DDY958, DDY950, DDY947, DDY952, and DDY1276. Strain details are in Table S1 in File S1.

cyan fluorescent protein (clone W7) (Heim and Tsien 1996) and Cdc13 with yellow fluorescent protein (clone 10C) (Ormö *et al.* 1996; Khadaroo *et al.* 2009). Fluorophores were visualized with oil immersion on a widefield microscope (AxioImager Z1; Carl Zeiss, Thornwood, NY) equipped with a $100\times$ objective lens (Plan Apochromat, numerical aperture 1.4; Carl Zeiss), a cooled charge-coupled device camera (Orca-ER; Hamamatsu Photonics), DIC, and an illumination source (HXP120C; Carl Zeiss). Eleven optical sections with 0.4 μm spacing through the cell were imaged. Images were acquired and analyzed using Volocity software (PerkinElmer). Images were pseudocolored according to the approximate emission wavelength of the fluorophores.

Data availability

The authors state that all data necessary for confirming the conclusions presented in the article are represented fully within the article. Table S1 in File S1 lists all strains.

Results

dna2Δ lethality is suppressed by checkpoint inactivation

To clarify the effect of DNA damage checkpoint gene deletions in *dna2Δ* cells, heterozygous *dna2Δ checkpointΔ* diploid

strains were sporulated, tetrads were dissected, and viable genotypes determined. We examined the effects of *RAD9*, *DDC1*, and *MEC1*, affecting a checkpoint mediator protein, a component of the 9-1-1 checkpoint sliding clamp, and the central checkpoint kinase (homolog of human ATR), respectively, and all previously studied in the context of *dna2Δ* (Budd *et al.* 2011; Kumar and Burgers 2013). We also examined *RAD17*, encoding a partner of Ddc1 in the checkpoint sliding clamp; *CHK1*, encoding a downstream checkpoint kinase; *RAD53*, a parallel downstream kinase; and *TEL1*, encoding the homolog of human ATM. As a positive control for suppression, we also examined the effects of *PIF1*, encoding a 5′ to 3′ helicase, because *pif1Δ* (like *rad9Δ*) suppresses *dna2Δ* (Budd *et al.* 2006).

dna2Δ rad9Δ and *dna2Δ pif1Δ* strains are temperature sensitive (Budd *et al.* 2006, 2011) and therefore spores were germinated at 20, 23, and 30° to allow comparison of *dna2Δ* suppression frequencies at different temperatures. Interestingly, the effects of *rad9Δ*, *ddc1Δ*, *rad17Δ*, *chk1Δ*, and *mec1Δ* were very similar, as they each permitted *dna2Δ* strains to form colonies at 20 and 23° but not at 30° (Figure 1, Figure S1a in File S1, and Table 1). In comparison, *pif1Δ* suppressed *dna2Δ* with higher efficiency and at higher temperatures, and *pif1Δ dna2Δ* colonies on germination plates were larger than those permitted by checkpoint gene deletions (Figure 1,

Table 1 dna2Δ suppression efficiency

	20°		23°		30°	
	Viable dna2Δ xyzΔ	Expected dna2Δ xyzΔ	Viable dna2Δ xyzΔ	Expected dna2Δ xyzΔ	Viable dna2Δ xyzΔ	Expected dna2Δ xyzΔ
XYZ	0	12			0	12
rad9Δ	14	26	7	26	0	25
ddc1Δ	13	26	11	26	0	26
rad17Δ	20	23	12	26	0	25
chk1Δ	14	26	7	25	0	26
mec1Δ sml1Δ	16	49			0	12
pif1Δ	24	25			13	12
mph1Δ	10	26			0	13
pol32Δ	0	13	5	13	9	13
rad53Δ sml1Δ	0	19			0	25
tel1Δ	0	38			0	13
sml1Δ	0	13				

20, 23, and 30° are the temperatures at which spores were germinated. The leftmost column shows the gene deleted in each dna2Δ/+ diploid. Viable dna2Δ xyzΔ is the number of spores that germinated and formed visible colonies. Expected dna2Δ xyzΔ is the expected number of viable dna2Δ xyzΔ strains if xyzΔ completely suppressed the dna2Δ inviable phenotype, based on the total number of tetrads dissected. For example, 25% of dna2Δ/+ rad9Δ/+ spores should be dna2Δ rad9Δ, and 12.5% of mec1Δ/+ sml1Δ/+ dna2Δ/+ should be mec1Δ sml1Δ dna2Δ.

Figure S1a in File S1, and Table 1). tel1Δ and rad53Δ did not suppress dna2Δ, presumably because they have different roles in the DNA damage response. We conclude that rad9Δ, ddc1Δ, rad17Δ, chk1Δ, and mec1Δ, but not rad53Δ and tel1Δ checkpoint mutations, suppress inviability caused by dna2Δ. These data suggest that dna2Δ causes lethal Rad9, Rad17, Ddc1, Chk1, and Mec1 mediated cell-cycle arrest. Given that checkpoint mutations suppress dna2Δ and telomere defects (cdc13-1, yku70Δ, and stn1-13) (Addinall et al. 2008; Holstein et al. 2017) but enhance DNA replication defects (Weinert et al. 1994; Dubarry et al. 2015), the pattern of dna2Δ genetic interactions strongly suggests that dna2Δ cells contain telomere defects.

DNA2 deletion causes temperature sensitivity

On germination plates dna2Δ checkpointΔ colonies were often small and heterogeneous in size in comparison with dna2Δ pif1Δ colonies, implying that mutating checkpoint genes did not suppress the dna2Δ growth defects as efficiently as removing the Pif1 helicase (Figure 1). One explanation for this difference in colony size was that checkpoint mutations permitted only a limited number of cell divisions, but that ultimately the dna2Δ checkpointΔ double-mutant clones would senesce and cease growth. To test this hypothesis, dna2Δ checkpointΔ double mutants were passaged further. Interestingly, the opposite to senescence was observed, and dna2Δ checkpointΔ mutants in fact became fitter and more homogeneous in colony size with passage and grew indefinitely (Figure 2A and Figure S2a in File S1). This suggests that dna2Δ checkpointΔ double mutants originally grow quite poorly and that some type of adaptation to the absence of Dna2 occurs in dna2Δ checkpointΔ mutants. We considered that additional suppressor mutations had arisen in dna2Δ checkpointΔ mutants, but backcross experiments did not support this hypothesis (Figure S1b in File S1). It was also clear that even different strains of the same genotype became

similarly fit when passaged at 23°, which is inconsistent with different suppressor mutations arising. However, all strains remained temperature sensitive for growth at higher temperatures, and growth at high temperature was more heterogeneous than growth at low temperature (Figure 2B and Figure S2b in File S1). Overall, passage of dna2Δ checkpointΔ strains shows that they adapt to the absence of Dna2 but remain temperature sensitive for growth, presumably because ongoing cellular defects are more penetrant at higher temperature. Consistent with a previous study (Budd et al. 2006), dna2Δ pif1Δ strains, the least temperature-sensitive genotype, formed smaller colonies at 36° than at 30°, showing that even these cells also have a temperature-sensitive molecular defect (Figure 2B). We noted a similarity between yku70Δ and dna2Δ strains as each genotype exhibits a temperature-sensitive phenotype and is suppressed by checkpoint mutations (Maringele and Lydall 2002). In the case of yku70Δ mutants, high levels of 3′ ssDNA are generated at telomeres at high temperature (Maringele and Lydall 2002).

dna2Δ cells have abnormal telomere length with limited ssDNA

We next tested whether Dna2 affects the structure of telomeric DNA. We first tested for increased levels of 3′ ssDNA at telomeres in dna2Δ cells because this is seen in yku70Δ cells (Maringele and Lydall 2002). Furthermore, in fission yeast, Dna2 was shown to be involved in the generation of G-rich ssDNA at telomeres (Tomita et al. 2004). Importantly, it was reported that dna2Δ rad9Δ cells have abnormally low levels of telomeric 3′ G-rich ssDNA (Budd and Campbell 2013). Consistent with what was reported for rad9Δ dna2Δ, chk1Δ dna2Δ, mec1Δ dna2Δ, rad17Δ dna2Δ, ddc1Δ dna2Δ, and pif1Δ dna2Δ cells all showed low levels of 3′ G-rich ssDNA at telomeres in comparison with DNA2 strains (Figure 3, A and B and Figures S3 and S4 in File S1). We conclude that all
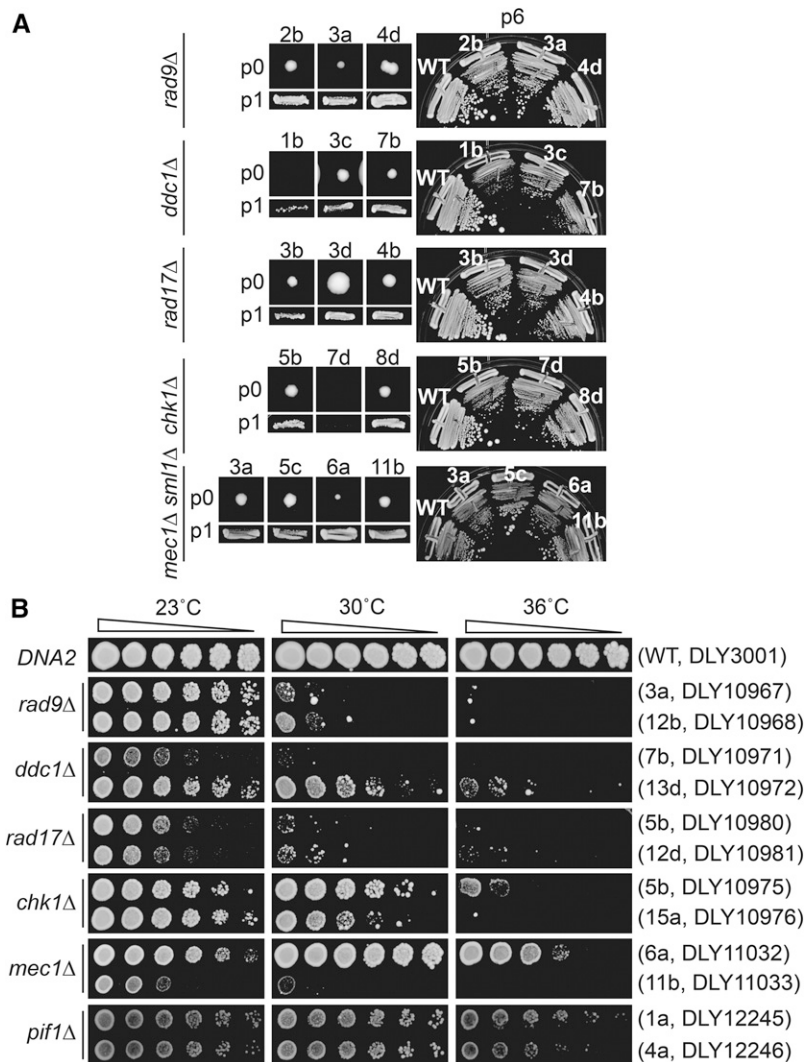
Figure 2 *dna2Δ* strains improve growth with passage, but remain temperature sensitive. (A) Colonies of *dna2Δ yfgΔ* double mutants on germination plates (passage 0, p0) p1 (patched) and p6 (streaked) are shown. A single DNA2 (wild type; WT) is used for comparison at p6. (B) Spot test assays of strains at p6 (or p1 for *pif1Δ dna2Δ* strain). Strains of each genotype at each temperature were grown on single agar plates, but images have been cut and pasted to make comparisons easier. Original images are in Figure S2 in File S1. Each colony position on germination plates from Figure 1 and strain numbers are indicated. Strain details are in Table S1 in File S1.

dna2Δ mutants have low levels of telomeric 3′ ssDNA. Interestingly, the *dna2Δ* ssDNA phenotype is opposite to that observed in other telomere-defective strains (*cdc13-1* and *yku70Δ* mutants), which contain high levels of 3′ telomeric ssDNA (Maringele and Lydall 2002). We also checked for 5′ C-rich ssDNA and saw no evidence for increased levels of telomeric C-rich ssDNA (Figure S5 in File S1).

To search for other telomeric DNA phenotypes in *dna2Δ* strains, we examined telomere length by Southern blotting. Interestingly, the telomeres of *chk1Δ dna2Δ*, *mec1Δ dna2Δ*, *rad17Δ dna2Δ*, and *ddc1Δ dna2Δ* cells were long, and in fact longer and more diffuse than *pif1Δ* strains, known to have very long telomeres (Schulz and Zakian 1994) (Figure 3C and Figures S4 and S6 in File S1). In contrast, and as reported before, *rad9Δ dna2Δ* telomeres were slightly shorter than the wild-type length (Budd and Campbell 2013). Rad9 is unique among checkpoint proteins because it binds chromatin and inhibits nuclease activity at telomeres and DSBs (Bonetti *et al.* 2015; Ngo and Lydall 2015). Perhaps, therefore, the comparatively short telomere length in *rad9Δ dna2Δ* mutants reflects this chromatin-binding function of Rad9 at telomeres.

In summary, all *dna2Δ* mutants analyzed have abnormal telomere lengths and low levels of 3′ G-rich ssDNA.

Long telomeres are present in telomerase-deficient, recombination (*RAD52*)-dependent survivors (Wellinger and Zakian 2012). Recombination is also important to rescue stalled replication forks in telomeric sequences because the terminal location of telomeric DNA means that stalled forks cannot be rescued by forks arriving in the opposite direction, as in elsewhere in the genome. Because the telomeres in *dna2Δ* strains were often long, we wondered if recombination contributed to the viability of *dna2Δ* strains. Interestingly, Rad52 did seem to contribute to the viability of *rad9Δ dna2Δ* and *ddc1Δ dna2Δ* strains (Figure S7 in File S1). This strongly suggests that recombination-dependent mechanisms help *dna2Δ* cells maintain viability.

Dna2 nuclease is critical in checkpoint-defective cells

Dna2 is a nuclease as well as a helicase, and directly activates the central checkpoint kinase Mec1 (Kumar and Burgers 2013). Any of these functions might be important at telomeres or elsewhere. To test which biochemical activity is
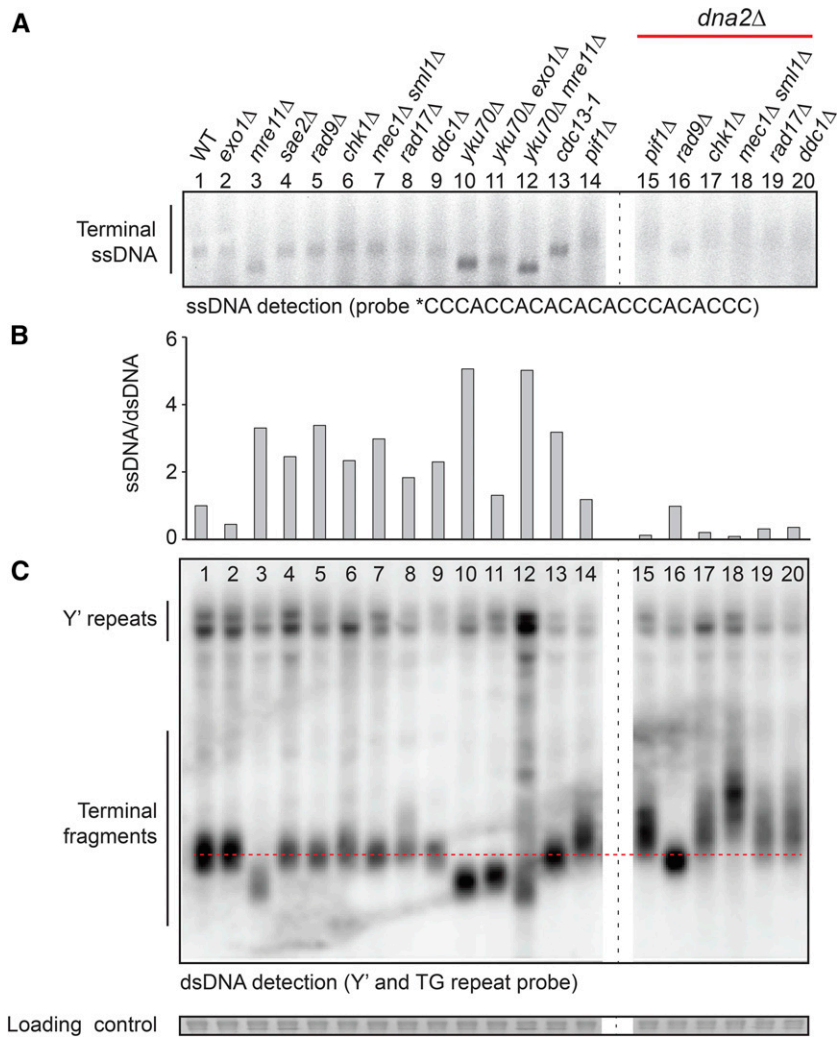
Figure 3 Telomeres of *dna2Δ* strains are abnormal and have low levels of ssDNA. (A) An in-gel assay was performed to measure telomeric ssDNA. Saturated cultures were diluted at 1:25 (*dna2Δ* strains) or 1:50 (other strains) and grown for 6 hr until a concentration of ~10⁷ cells/ml was attained. DNA was isolated from *dna2Δ* strains at passage 6, except for *dna2Δ pif1Δ* strain which is of unknown passage number. Strains were as follows: wild type (WT) (DLY3001), *exo1Δ* (DLY1272), *mre11Δ* (DLY4457), *sae2Δ* (DLY1577), *rad9Δ* (DLY9593), *chk1Δ* (DLY10537), *mec1Δ sml1Δ* (DLY1326), *rad17Δ* (DLY7177), *ddc1Δ* (DLY8530), *yku70Δ* (DLY6885), *yku70Δ exo1Δ* (DLY1408), *yku70Δ mre11Δ* (DLY1845), *cdc13-1* (DLY1108), *pif1Δ* (DLY4872), *pif1Δ dna2Δ* (DLY4690), *rad9Δ dna2Δ* (DLY10967), *chk1Δ dna2Δ* (DLY10975), *mec1Δ sml1Δ dna2Δ* (DLY11032), *rad17Δ dna2Δ* (DLY10981), and *ddc1Δ dna2Δ* (DLY10973). Strain details are in Table S1 in File S1. * indicates a 5′ IRDye 800 label. (B) ssDNA and double-stranded DNA (dsDNA) were quantified using ImageJ analysis of the images shown in A and C. The ratio of ssDNA/dsDNA was plotted and the wild-type strain was given the value of "1"; all other ratios are expressed relative to the wild type. The telomeric regions quantified are indicated in Figure S3 in File S1. Analysis of independent strains of the same genotypes is shown in Figure S4 in File S1. (C) Southern blotting was performed to measure telomeric dsDNA with a Y′-TG probe. SYBR Safe was used as a loading control, as previously described (Holstein *et al.* 2014).

most important to cell fitness, we transformed nuclease-, helicase-, or checkpoint-defective alleles of *DNA2* into *rad9Δ dna2Δ* or *ddc1Δ dna2Δ* cells, and measured growth at high temperature. It was clear that helicase dead and checkpoint-defective alleles rescued the *dna2Δ* defect and permitted growth at high temperatures (Figure 4B and Figure S8 in File S1). In contrast, the nuclease-defective allele of *DNA2* did not rescue the *dna2Δ* growth defect. We conclude that the most critical function of Dna2 in checkpoint-defective yeast cells is its nuclease function.

dna2Δ mutants contain RPA-bound telomeres

dna2Δ cells are temperature sensitive, have telomere length phenotypes, and stimulate checkpoint pathways. However, paradoxically, *dna2Δ* cells have reduced levels of telomeric ssDNA when measured by in-gel assay. We reasoned that one plausible function for Dna2 nuclease activity was removal of ssDNA present *in vivo* that was not detectable *in vitro*. That is, unwound terminal telomeric DNA formed Y-shaped structures *in vivo*, with splayed arms of G-rich and C-rich ssDNA. The 5′ C-rich and 3′ G-rich ssDNA should bind RPA and CST (Cdc13, Stn1, and Ten1) (Nugent *et al.* 1996), respectively,

with the RPA-coated 5′ ssDNA stimulating DNA damage checkpoint pathways. The ssDNA present on the arms of Y-shaped telomeres *in vivo* might not be detected by in-gel assays because complementary ssDNA strands would reanneal during DNA purification. Finally, telomere unwinding might be catalyzed by helicases (for example, Pif1) and high temperature, explaining the effects of *pif1Δ* and temperature on fitness of *dna2Δ* cells.

Most eukaryotic cells contain 3′ ssDNA overhangs on the G-rich strand of telomeric DNA, and this ssDNA is bound by proteins such as Pot1 and CST. If unwound telomeres occur in *dna2Δ* cells, then CST should still bind the 3′ strand, but in addition, RPA could bind the C-rich 5′ strand and stimulate the checkpoint. Presumably, in such a case, both RPA and CST complexes would colocalize at telomeres and stop the stimulation of the checkpoint pathway. To explore RPA and CST localization, the two largest subunits of each complex, Cdc13 and Rfa1, were tagged with yellow and cyan fluorescent proteins, respectively, and their localization in *dna2Δ* cells was examined by live-cell microscopy.

We examined Cdc13 and Rfa1 foci in *ddc1Δ dna2Δ*, *pif1Δ dna2Δ* cells and wild-type, *ddc1Δ*, *pif1Δ* controls. Because
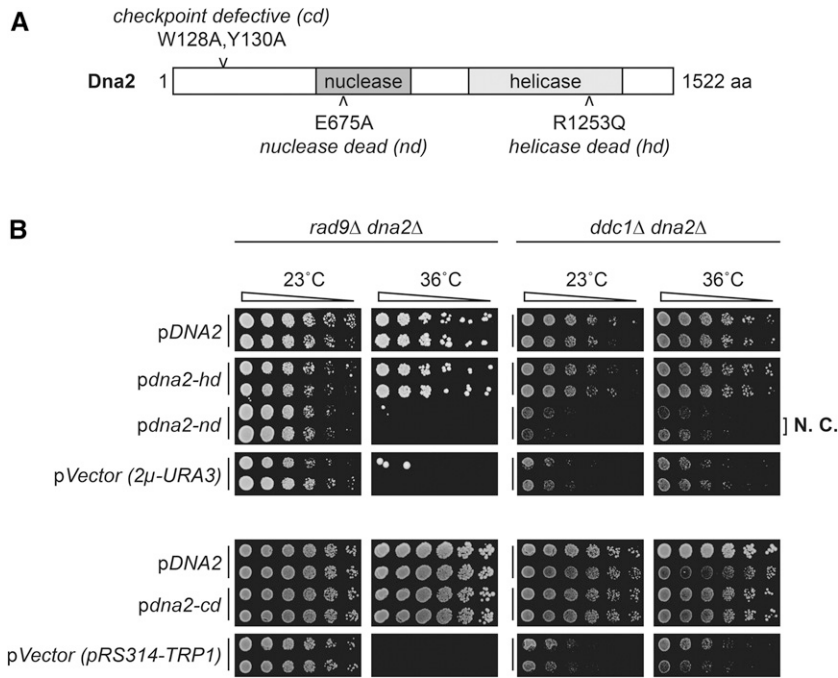
Figure 4 The nuclease domain of Dna2, but not helicase or checkpoint domains, confers viability of *dna2Δ* strains. (A) Domain structure of yeast Dna2. Mutations affecting checkpoint, nuclease, and helicase domains are indicated. (B) Spot test assay performed as in Figure 2B. Strains from passage 6 of original colony 3a (*rad9Δ dna2Δ*, DLY10967), and 13d (*ddc1Δ dna2Δ*, DLY10973) were used for plasmid transformation. *rad9Δ dna2Δ* and *ddc1Δ dna2Δ* strains carrying *DNA2*, empty vector or helicase-dead, nuclease-dead or checkpoint-dead alleles of *DNA2* were inoculated into 2 ml –URA or –TRP media for plasmid selection and cultured for 48 hr, at 23°. Original images are in Figure S8 in File S1. Strain details are in Table S1 in File S1. Plasmid details are in Table S2 in File S1. N.C., no complementation.

some of these cells grew poorly and may have altered cell-cycle distributions, we counted foci in budded cells (S/G2/M) as this is when RPA foci are more likely to be present (Figure 5). We observed broadly similar fractions of cells with Cdc13 foci in all cultures at the level of 30–70%, but checkpoint-defective strains *ddc1Δ* and *ddc1Δ dna2Δ* had somewhat higher levels (closer to 70%) (Figure 5A). In G1 cells the number of Cdc13 foci was smaller (<20%), but *ddc1Δ dna2Δ* cells tended to have consistently slightly higher levels (on average 15%) (Figure S9a in File S1). We conclude that *DNA2* deletion has no strong effect on Cdc13 foci formation.

We also searched for Rfa1 foci and observed that, on average, 30% of budded and 10% of unbudded control cells contained Rfa1 foci (Figure 5B and Figure S9b in File S1). In contrast, *ddc1Δ dna2Δ* and *pif1Δ dna2Δ* cultures contained a much higher fraction of budded cells with Rfa1 foci. Generally, >80% of *ddc1Δ dna2Δ* and *pif1Δ dna2Δ* cells, and ~40% of *pif1Δ* cells contained at least one Rfa1 focus (Figure 5B), suggesting that high levels of DNA damage and ssDNA are present in these strains. In G1 cells, the number of Rfa1 foci was smaller (up to 80%), and cells hardly ever contained more than one Rfa1 focus (Figure S9b in File S1).

If the Rfa1 foci observed in *dna2Δ* cells were primarily at telomeres, rather than at DSBs or long flaps on Okazaki fragments elsewhere in the genome, then Rfa1 foci in *dna2Δ* cells should preferentially localize at telomeres. Assuming Cdc13 foci are at telomeres (Khadaroo *et al.* 2009), then >60% of these telomeric loci in *ddc1Δ dna2Δ* budded cells colocalized with Rfa1 (Figure 5C). In contrast, <10% of Cdc13 foci contained Rfa1 in wild-type or *ddc1Δ* budded cells, suggesting low Rfa1 at telomeres in wild-type and *ddc1Δ* strains. This suggests that RPA-bound ssDNA occurs at high frequency near telomeres in *ddc1Δ dna2Δ* cells. *pif1Δ dna2Δ* cells contained

nearly as many Rfa1 foci and Cdc13 foci as *ddc1Δ dna2Δ* cells, but less Cdc13 foci contained Rfa1 (~30%). We conclude that *pif1Δ dna2Δ* cells have less RPA-bound ssDNA at telomeres than *ddc1Δ dna2Δ* cells. Interestingly, *pif1Δ* single mutants also contained more Rfa1 foci than wild-type cells, and more colocalization of Rfa1 and Cdc13 (~5%) (Figure 5, B–D). This suggests that *pif1Δ* cells, which contain long telomeres, show comparatively high levels of RPA binding at telomeres, possibly due to the difficulty of replicating through long stretches of telomeric DNA.

Overall, of all the genotypes examined, *ddc1Δ dna2Δ* mutants had the highest fraction of Cdc13 foci that contain Rfa1, Rfa1 foci that contain Cdc13, and Cdc13-Rfa1 foci (Figure 5, C and D and Figure S9f in File S1). These data are consistent with a model in which both G-rich and C-rich ssDNA are found at high levels at telomeres in *ddc1Δ dna2Δ* cells. Interestingly, *pif1Δ dna2Δ* cells also contained increased levels of CST/RPA-bound ssDNA, suggesting that Pif-independent helicases may unwind telomeric C-rich and G-rich ssDNA in the absence of Pif1, to generate substrates for RPA binding.

dna2Δ lethality is suppressed by *mph1Δ* and *pol32Δ*, but not *sgs1Δ*

To search for additional activities that might unwind telomeric DNA, like Pif1, we examined genes affecting likely candidates. Sgs1 was a candidate since it functions with Dna2 in resection of DSBs and uncapped telomeres (Cejka *et al.* 2010; Ngo *et al.* 2014), but its deletion did not suppress *dna2Δ* (Figure S10a in File S1), as has been reported by others (Hoopes *et al.* 2002; Weitao *et al.* 2003; Budd *et al.* 2005). On this basis Sgs1 does not seem to contribute to telomere unwinding, or if it does, it also has other functions that are essential in *dna2Δ* strains.
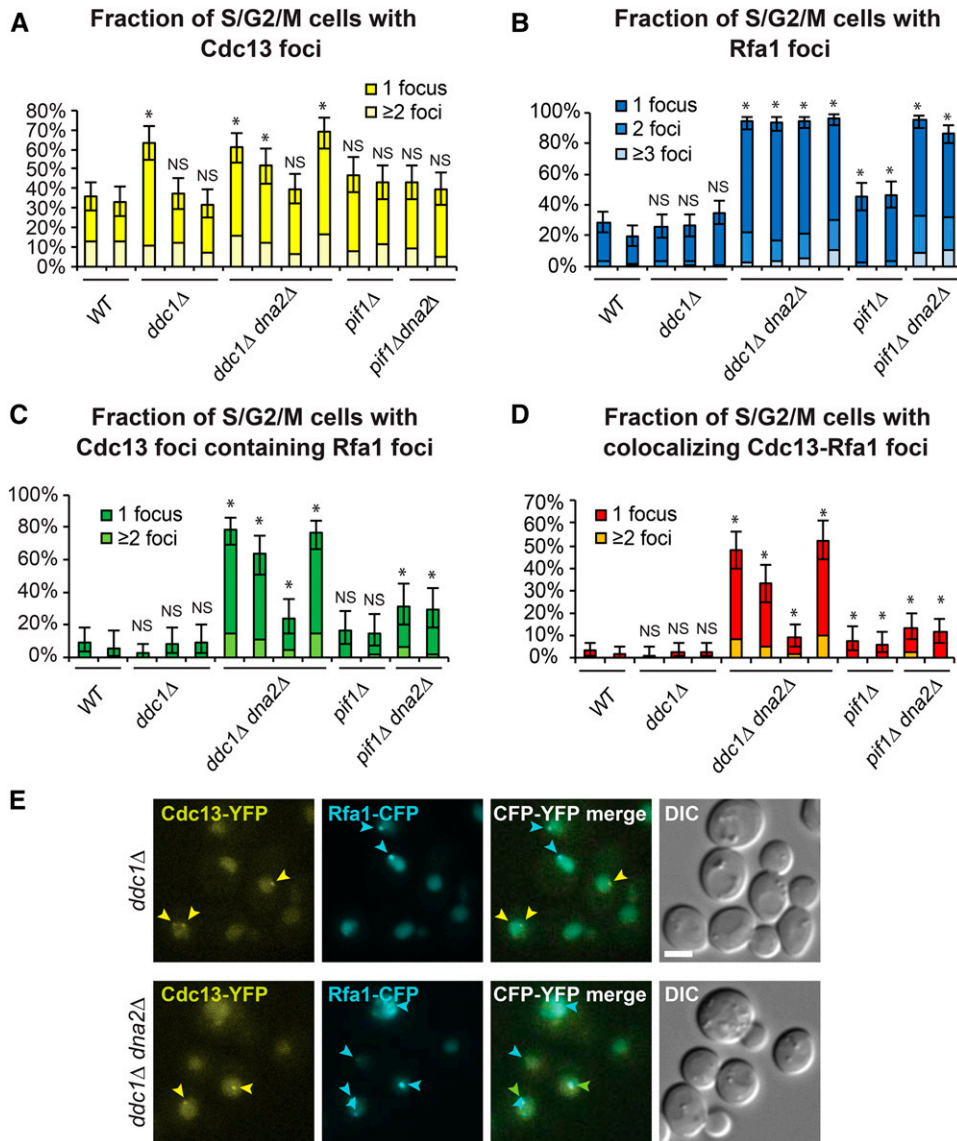
Figure 5 dna2Δ mutants accumulate CST and RPA, the ssDNA binding complexes. (A–D) Percentages of Cdc13 foci, Rfa1 foci, or colocalized Cdc13-Rfa1 foci in dna2Δ and control strains are shown. (A) Percentage of budded (S/G2/M) cells with either Cdc13 foci only or Cdc13-Rfa1 foci. (B) Percentage of budded cells with either Rfa1 foci only or Cdc13-Rfa1 foci. (C) Percentage of budded cells with Cdc13 foci that colocalize with Rfa1 foci. (D) Percentage of budded cells with colocalizing Cdc13-Rfa1 foci. Error bars indicate 95% confidence intervals (n = 213–437, from two independent cultures of each strain). * indicates statistical significance (P < 0.05) determined using Fisher's exact test. Strains are as follows: wild type (WT) (DLY12342, DLY12343), ddc1Δ (DLY12282, DLY12280, DLY12283), ddc1Δ dna2Δ (DLY12281, DLY12341, DLY12284, DLY12279), pif1Δ (DLY12346, DLY12347), and pif1Δ dna2Δ (DLY12344, DLY12345). (E) An example of live-cell images is shown. Cdc13-Rfa1 colocalized foci are indicated by green arrows, Cdc13 foci by yellow arrows, and Rfa1 foci by blue arrows. Bar, 3 μm. Strain details are in Table S1 in File S1.

We examined Mph1, because like Pif1, Mph1 stimulates Dna2 activity on 5′ flaps in vitro (Kang et al. 2009). Interestingly, mph1Δ suppressed dna2Δ. The effect of mph1Δ was similar to checkpoint mutations, but not as strong as pif1Δ (Figure S10, a–c in File S1). Therefore loss of Mph1, a 3′ to 5′ helicase, like loss of Pif1, a 5′ to 3′ helicase, suppresses the inviability of dna2Δ cells. Given the polarity of the Mph1 helicase, it would most likely engage with the 3′ G-rich overhanging strand to unwind telomeric DNA, and compete with CST for this substrate. To test this hypothesis, mph1Δ was combined with cdc13-1 and the temperature-sensitive phenotype was scored. Interestingly, mph1Δ mildly suppresses the temperature-dependent growth defects of cdc13-1 mutants (Figure S10d in File S1). This suggests that Mph1 and CST compete to bind the same G-rich strand at telomeres, and is consistent with the idea that Mph1 engages with the 3′ telomeric overhang to unwind telomeric double-stranded DNA.

Finally, we tested Pol32, a DNA Pol δ subunit, which helps displace 5′ ends of Okazaki fragments. It had been reported that pol32Δ suppresses some alleles of DNA2, and weakly suppresses dna2Δ (Budd et al. 2006; Stith et al. 2008). Interestingly, we confirmed that pol32Δ suppressed dna2Δ. In contrast to checkpoint mutations, pol32Δ suppressed dna2Δ at high temperature (30° and 23°) but not at 20° (Figure S10, a–c in File S1). This temperature-dependent suppression may be explained by the fact that pol32Δ mutants are cold sensitive (Gerik et al. 1998).

Discussion

We report that loss of proteins affecting numerous aspects of the DNA damage response permit budding yeast cells to divide indefinitely in the absence of the essential protein Dna2. Loss of DNA damage checkpoint proteins (Rad9, Ddc1, Rad17, Chk1, and Mec1) or Pif1, a 5′ to 3′ helicase, Mph1, a 3′ to 5′ helicase, or Pol32, a DNA polymerase δ subunit, suppress the inviability of dna2Δ cells. The suppression of dna2Δ by checkpoint mutations makes dna2Δ mutants more similar to telomere-defective
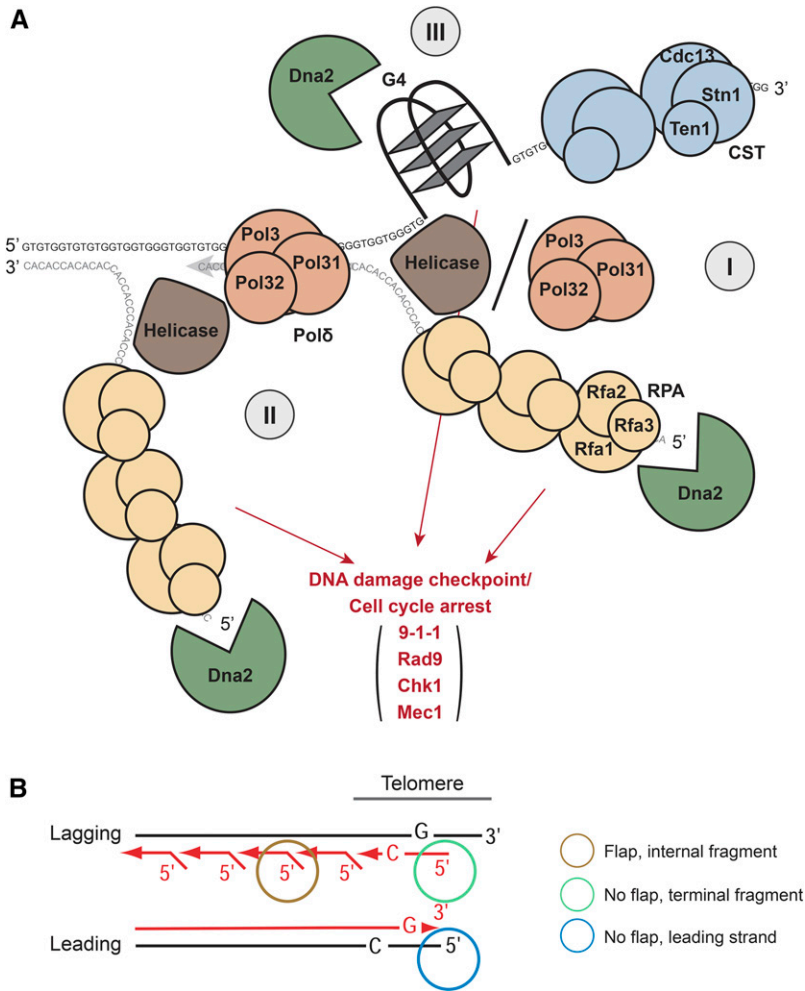
Figure 6 Three plausible roles for Dna2 in removing unwound RPA-coated ssDNA at telomeres. (A) Three scenarios for Dna2 activity. Scenario I: 5′ RPA-coated ssDNA cleavage at telomeric termini. Telomere ends are unwound by helicases, for example, Pif1 or Mph1. The 3′ G-rich strand is bound by CST and the 5′ C-rich strand is bound by RPA, a substrate for Dna2 cleavage. Scenario II: Processing of long flaps on Okazaki fragments near telomeres. DNA polymerase δ displacement activity, stimulated by helicase(s), generates long flaps on an Okazaki fragment near telomere. Long C-rich flap, bound by RPA, are subjected to Dna2 cleavage. Scenario III: G-quadruplex unwinding and processing. G-quadruplexes formed on telomeric G-rich ssDNA are unwound or processed by Dna2. All proteins were drawn to scale. (B) Lagging and leading strand replication at telomeres. Short red arrows indicate Okazaki fragments on the lagging strand. The long red arrow indicates replicated leading strand. The brown circle indicates the flap formed on an internal Okazaki fragment. The green circle indicates no flap on the terminal telomeric Okazaki fragment. The blue circle indicates no flap on the leading strand template.

strains than general DNA replication-defective strains (Dubarry *et al.* 2015). Consistent with this, *dna2*Δ strains show telomere length phenotypes and a high degree of colocalization of Cdc13, a telomeric G-rich ssDNA binding protein, and Rfa1, a more general ssDNA binding protein *in vivo*. *dna2*Δ mutants are also temperature sensitive and have low levels of telomeric G-rich ssDNA. The nuclease function of Dna2, but not helicase and checkpoint functions, is critical to confer the viability of *dna2*Δ *checkpoint*Δ strains at high temperature.

The low levels of telomeric 3′ ssDNA that we detect at telomeres of *dna2*Δ mutants by *in vitro* in-gel assay is the opposite phenotype to the high levels of 3′ ssDNA found at telomeres in other telomere-defective strains suppressed by checkpoint gene mutations (for example, *cdc13-1* and *yku70*Δ mutants) (Maringele and Lydall 2002; Ngo *et al.* 2014). Our explanation is that high levels of RPA-coated C-rich ssDNA and comparatively normal levels of CST-coated G-rich ssDNA are present at unwound telomeres of *dna2*Δ cells *in vivo*. This is detected as colocalization by live-cell imaging, but when DNA is extracted, it renatures during purification and ssDNA is not detected.

There are at least three plausible scenarios for why Dna2 might have its most critical functions at or near telomeres

(Figure 6A). One model that best fits all our data is that Dna2 nuclease activity removes potentially harmful, RPA-coated 5′ C-rich ssDNA at the termini of telomeres (Figure 6A, scenario I). In this model, helicases like Pif1 or Mph1 unwind the telomeric termini. The G-rich strand is bound by the telomeric CST complex and is presumably quite benign, but the C-rich strand is bound by RPA and potentially stimulates DNA damage checkpoint activity. Pol32, a subunit of DNA polymerase δ with strand displacement activity (Podust *et al.* 1995; Maga *et al.* 2001), might also generate ssDNA at the telomeric terminus, if CST recruits Pol α for lagging strand fill-in, which in turn recruits Pol δ (Waga and Stillman 1998; Maga *et al.* 2000; Burgers 2009).

Another potential role for Dna2 at telomeres is in removing long flaps of subtelomeric Okazaki fragments (Figure 6A, scenario II). Finally, Dna2 nuclease activity may be needed at stalled replication forks in telomeric regions (Figure 6A, scenario III). For example, mammalian and yeast telomeres are G-rich, difficult to replicate, and can form G-quadruplexes that might be processed by Dna2 (Gilson and Geli 2007; Masuda-Sasa *et al.* 2008; Lin *et al.* 2013; Maestroni *et al.* 2017). At other genomic locations, other substrates for Dna2 (*e.g.*, DSBs or stalled replication forks) can also occur

(Hu *et al.* 2012; Ngo *et al.* 2014), but our evidence is that telomeres are particularly reliant on Dna2.

If Dna2 acts at the very termini of telomeres (Figure 6A, scenario I), either the lagging strand, the leading strand, or both might be targets for Dna2 (Figure 6B). It is well-established that the leading and lagging strands of telomeres are processed by different mechanisms (Parenteau and Wellinger 1999; Wu *et al.* 2012; Bonetti *et al.* 2013; Soudet *et al.* 2014). After lagging strand replication is complete, the very terminus cannot be fully replicated because of the end replication problem. Irrespective of whether the most terminal Okazaki fragment is created by passage of the replication fork or CST recruitment of Pol α, it is unusual as unlike >99% of the other Okazaki fragments, it will not contain a flap at its 5′ end (Figure 6B). Perhaps the absence of a flap and/or a polymerase facilitates helicase engagement. The leading strand telomere end, which is thought to be blunt after the replication fork has passed, may also be susceptible to helicase activities.

We and others (Budd and Campbell 2013) have shown that *dna2Δ rad9Δ* cells have a short telomere phenotype. All other *dna2Δ* strains, including other checkpoint-defective strains, have long telomeres. Hence it is not telomere length *per se* that determines the survival of *dna2Δ* cells. Rad9, like its human ortholog 53BP1, binds chromatin and inhibits resection at telomere-defective *cdc13-1* cells and at DSBs (Iwabuchi *et al.* 2003; Lazzaro *et al.* 2008; Bunting *et al.* 2010; Ngo and Lydall 2015). Perhaps Rad9 binding to chromatin also inhibits helicase activity, telomere unwinding, and nuclease activity. Presumably unwound telomeres are also more susceptible to nucleases (other than Dna2). Consistent with this, the 9-1-1 complex recruits Dna2 and Exo1 nuclease to uncapped telomeres (Ngo and Lydall 2015), and *ddc1Δ dna2Δ* and *rad17Δ dna2Δ* mutants, defective in 9-1-1, have long telomeres.

Telomeres in all organisms are difficult to replicate and need to be protected from the harmful aspects of the DNA damage response. Telomeric structures like t-loops, and proteins like CST, shelterin, and the Ku heterodimer may help protect telomeric DNA from being unwound by helicases. Our experiments in yeast suggest that Dna2 is critical for removing RPA-coated C-rich ssDNA at unwound telomeres. *DNA2* is an essential gene in budding and fission yeasts, *C. elegans*, mice, and human cells. Interestingly, *C. elegans dna2Δ* mutants show temperature-dependent delayed lethality (Lee *et al.* 2003), suggesting that temperature-dependent telomere unwinding in *C. elegans* creates substrates for Dna2 nuclease activity at high temperatures.

Dna2 localizes at telomeres in yeast, humans, and mice, and Dna2 affects telomere phenotypes in all these organisms (Choe *et al.* 2002; Lin *et al.* 2013). Dna2, checkpoint proteins, Pif1 and Mph1 helicases, and Pol32 are all conserved between human and yeast cells, and affect telomere-related human diseases such as cancer, suggesting our observations may be relevant to human disease (Paeschke *et al.* 2013; Byrd and Raney 2015; Ceccaldi *et al.* 2016). It will be interesting to see if telomere-specific functions for Dna2 are conserved across eukaryotes.

Literature Cited

Addinall, S. G., M. Downey, M. Yu, M. K. Zubko, J. Dewar *et al.*, 2008 A genomewide suppressor and enhancer analysis of cdc13–1 reveals varied cellular processes influencing telomere capping in Saccharomyces cerevisiae. Genetics 180: 2251–2266. https://doi.org/10.1534/genetics.108.092577

Bae, S. H., K. H. Bae, J. A. Kim, and Y. S. Seo, 2001 RPA governs endonuclease switching during processing of Okazaki fragments in eukaryotes. Nature 412: 456–461. https://doi.org/10.1038/35086609

Balakrishnan, L., and R. A. Bambara, 2013 Okazaki fragment metabolism. Cold Spring Harb. Perspect. Biol. 5: a010173.

Bonetti, D., M. Martina, M. Falcettoni, and M. P. Longhese, 2013 Telomere-end processing: mechanisms and regulation. Chromosoma 123: 57–66.

Bonetti, D., M. Villa, E. Gobbini, C. Cassani, G. Tedeschi *et al.*, 2015 Escape of Sgs1 from Rad9 inhibition reduces the requirement for Sae2 and functional MRX in DNA end resection. EMBO Rep. 16: 351–361. https://doi.org/10.15252/embr.201439764

Budd, M. E., and J. L. Campbell, 1997 A yeast replicative helicase, Dna2 helicase, interacts with yeast FEN-1 nuclease in carrying out its essential function. Mol. Cell. Biol. 17: 2136–2142. https://doi.org/10.1128/MCB.17.4.2136

Budd, M. E., and J. L. Campbell, 2013 Dna2 is involved in CA strand resection and nascent lagging strand completion at native yeast telomeres. J. Biol. Chem. 288: 29414–29429. https://doi.org/10.1074/jbc.M113.472456

Budd, M. E., W. C. Choe, and J. L. Campbell, 1995 DNA2 encodes a DNA helicase essential for replication of eukaryotic chromosomes. J. Biol. Chem. 270: 26766–26769. https://doi.org/10.1074/jbc.270.45.26766

Budd, M. E., A. H. Y. Tong, P. Polaczek, X. Peng, C. Boone *et al.*, 2005 A network of multi-tasking proteins at the DNA replication fork preserves genome stability. PLoS Genet. 1: e61.

Budd, M. E., C. C. Reis, S. Smith, K. Myung, and J. L. Campbell, 2006 Evidence suggesting that Pif1 helicase functions in DNA replication with the Dna2 helicase/nuclease and DNA polymerase delta. Mol. Cell. Biol. 26: 2490–2500. https://doi.org/10.1128/MCB.26.7.2490-2500.2006

Budd, M. E., I. A. Antoshechkin, C. Reis, B. J. Wold, and J. L. Campbell, 2011 Inviability of a DNA2 deletion mutant is due to the DNA damage checkpoint. Cell Cycle 10: 1690–1698. https://doi.org/10.4161/cc.10.10.15643

Bunting, S. F., E. Callen, N. Wong, H. T. Chen, F. Polato *et al.*, 2010 53BP1 inhibits homologous recombination in Brca1-deficient cells by blocking resection of DNA breaks. Cell 141: 243–254. https://doi.org/10.1016/j.cell.2010.03.012

Burgers, P. M., 2009 Polymerase dynamics at the eukaryotic DNA replication fork. J. Biol. Chem. 284: 4041–4045. https://doi.org/10.1074/jbc.R800062200

Byrd, A. K., and K. D. Raney, 2015 A parallel quadruplex DNA is bound tightly but unfolded slowly by pif1 helicase. J. Biol. Chem. 290: 6482–6494. https://doi.org/10.1074/jbc.M114.630749

Ceccaldi, R., P. Sarangi, and A. D. D'Andrea, 2016 The Fanconi anaemia pathway: new players and new functions. Nat. Rev. Mol. Cell Biol. 17: 337–349. https://doi.org/10.1038/nrm.2016.48

Cejka, P., E. Cannavo, P. Polaczek, T. Masuda-Sasa, S. Pokharel et al., 2010 DNA end resection by Dna2-Sgs1-RPA and its stimulation by Top3-Rmi1 and Mre11-Rad50-Xrs2. Nature 467: 112–116. https://doi.org/10.1038/nature09355

Chai, W., L. Zheng, and B. Shen, 2013 DNA2, a new player in telomere maintenance and tumor suppression. Cell Cycle 12: 1985–1986. https://doi.org/10.4161/cc.25306

Choe, W., M. Budd, O. Imamura, L. Hoopes, and J. L. Campbell, 2002 Dynamic localization of an Okazaki fragment processing protein suggests a novel role in telomere replication. Mol. Cell. Biol. 22: 4202–4217. https://doi.org/10.1128/MCB.22.12.4202-4217.2002

Dewar, J. M., and D. Lydall, 2010 Pif1- and Exo1-dependent nucleases coordinate checkpoint activation following telomere uncapping. EMBO J. 29: 4020–4034. https://doi.org/10.1038/emboj.2010.267

Dewar, J. M., and D. Lydall, 2012 Simple, non-radioactive measurement of single-stranded DNA at telomeric, sub-telomeric, and genomic loci in budding yeast. Methods Mol. Biol. 920: 341–348. https://doi.org/10.1007/978-1-61779-998-3_24

Dominguez-Valentin, M., C. Therkildsen, S. Veerla, M. Jonsson, I. Bernstein et al., 2013 Distinct gene expression signatures in lynch syndrome and familial colorectal cancer type x. PLoS One 8: e71755. https://doi.org/10.1371/journal.pone.0071755

Dubarry, M., C. Lawless, A. P. Banks, S. Cockell, and D. Lydall, 2015 Genetic networks required to coordinate chromosome replication by DNA polymerases alpha, delta, and epsilon in Saccharomyces cerevisiae. G3 5: 2187–2197. https://doi.org/10.1534/g3.115.021493

Duxin, J. P., B. Dao, P. Martinsson, N. Rajala, L. Guittat et al., 2009 Human Dna2 is a nuclear and mitochondrial DNA maintenance protein. Mol. Cell. Biol. 29: 4274–4282. https://doi.org/10.1128/MCB.01834-08

Gerik, K. J., X. Li, A. Pautz, and P. M. Burgers, 1998 Characterization of the two small subunits of Saccharomyces cerevisiae DNA polymerase delta. J. Biol. Chem. 273: 19747–19755. https://doi.org/10.1074/jbc.273.31.19747

Gilson, E., and V. Geli, 2007 How telomeres are replicated. Nat. Rev. Mol. Cell Biol. 8: 825–838. https://doi.org/10.1038/nrm2259

Heim, R., and R. Y. Tsien, 1996 Engineering green fluorescent protein for improved brightness, longer wavelengths and fluorescence resonance energy transfer. Curr. Biol. 6: 178–182. https://doi.org/10.1016/S0960-9822(02)00450-5

Holstein, E. M., K. R. Clark, and D. Lydall, 2014 Interplay between nonsense-mediated mRNA decay and DNA damage response pathways reveals that Stn1 and Ten1 are the key CST telomere-cap components. Cell Rep. 7: 1259–1269. https://doi.org/10.1016/j.celrep.2014.04.017

Holstein, E. M., G. Ngo, C. Lawless, P. Banks, M. Greetham et al., 2017 Systematic analysis of the DNA damage response network in telomere defective budding yeast. G3 7: 2375–2389. https://doi.org/10.1534/g3.117.042283

Hoopes, L. L. M., M. Budd, W. Choe, T. Weitao, and J. L. Campbell, 2002 Mutations in DNA replication genes reduce yeast life span. Mol. Cell. Biol. 22: 4136–4146. https://doi.org/10.1128/MCB.22.12.4136-4146.2002

Hu, J., L. Sun, F. Shen, Y. Chen, Y. Hua et al., 2012 The intra-S phase checkpoint targets Dna2 to prevent stalled replication forks from reversing. Cell 149: 1221–1232. https://doi.org/10.1016/j.cell.2012.04.030

Iwabuchi, K., B. P. Basu, B. Kysela, T. Kurihara, M. Shibata et al., 2003 Potential role for 53BP1 in DNA end-joining repair through direct interaction with DNA. J. Biol. Chem. 278: 36487–36495. https://doi.org/10.1074/jbc.M304066200

Jia, P. P., M. Junaid, Y. B. Ma, F. Ahmad, Y. F. Jia et al., 2017 Role of human DNA2 (hDNA2) as a potential target for cancer and other diseases: a systematic review. DNA Repair (Amst.) 59: 9–19. https://doi.org/10.1016/j.dnarep.2017.09.001

Kang, H. Y., E. Choi, S. H. Bae, K. H. Lee, B. S. Gim et al., 2000 Genetic analyses of Schizosaccharomyces pombe dna2(+) reveal that dna2 plays an essential role in Okazaki fragment metabolism. Genetics 155: 1055–1067.

Kang, Y. H., M. J. Kang, J. H. Kim, C. H. Lee, I. T. Cho et al., 2009 The MPH1 gene of Saccharomyces cerevisiae functions in Okazaki fragment processing. J. Biol. Chem. 284: 10376–10386. https://doi.org/10.1074/jbc.M808894200

Kao, H. I., and R. A. Bambara, 2003 The protein components and mechanism of eukaryotic Okazaki fragment maturation. Crit. Rev. Biochem. Mol. Biol. 38: 433–452. https://doi.org/10.1080/10409230390259382

Khadaroo, B., M. T. Teixeira, P. Luciano, N. Eckert-Boulet, S. M. Germann et al., 2009 The DNA damage response at eroded telomeres and tethering to the nuclear pore complex. Nat. Cell Biol. 11: 980–987. https://doi.org/10.1038/ncb1910

Kumar, S., and P. M. Burgers, 2013 Lagging strand maturation factor Dna2 is a component of the replication checkpoint initiation machinery. Genes Dev. 27: 313–321. https://doi.org/10.1101/gad.204750.112

Kumar, S., X. Peng, J. Daley, L. Yang, J. Shen et al., 2017 Inhibition of DNA2 nuclease as a therapeutic strategy targeting replication stress in cancer cells. Oncogenesis 6: e319. https://doi.org/10.1038/oncsis.2017.15

Lazzaro, F., V. Sapountzi, M. Granata, A. Pellicioli, M. Vaze et al., 2008 Histone methyltransferase Dot1 and Rad9 inhibit single-stranded DNA accumulation at DSBs and uncapped telomeres. EMBO J. 27: 1502–1512. https://doi.org/10.1038/emboj.2008.81

Lee, K. H., M. H. Lee, T. H. Lee, J. W. Han, Y. J. Park et al., 2003 Dna2 requirement for normal reproduction of Caenorhabditis elegans is temperature-dependent. Mol. Cells 15: 81–86.

Lee, S. E., J. K. Moore, A. Holmes, K. Umezu, R. D. Kolodner et al., 1998 Saccharomyces Ku70, mre11/rad50 and RPA proteins regulate adaptation to G2/M arrest after DNA damage. Cell 94: 399–409. https://doi.org/10.1016/S0092-8674(00)81482-8

Levikova, M., and P. Cejka, 2015 The Saccharomyces cerevisiae Dna2 can function as a sole nuclease in the processing of Okazaki fragments in DNA replication. Nucleic Acids Res. 43: 7888–7897. https://doi.org/10.1093/nar/gkv710

Levikova, M., D. Klaue, R. Seidel, and P. Cejka, 2013 Nuclease activity of Saccharomyces cerevisiae Dna2 inhibits its potent DNA helicase activity. Proc. Natl. Acad. Sci. USA 110: E1992–E2001. https://doi.org/10.1073/pnas.1300390110

Lin, W., S. Sampathi, H. Dai, C. Liu, M. Zhou et al., 2013 Mammalian DNA2 helicase/nuclease cleaves G-quadruplex DNA and is required for telomere integrity. EMBO J. 32: 1425–1439. https://doi.org/10.1038/emboj.2013.88

Lydall, D., and T. Weinert, 1995 Yeast checkpoint genes in DNA damage processing: implications for repair and arrest. Science 270: 1488–91.

Maestroni, L., S. Matmati, and S. Coulon, 2017 Solving the telomere replication problem. Genes (Basel) 8: 55.

Maga, G., M. Stucki, S. Spadari, and U. Hubscher, 2000 DNA polymerase switching: I. Replication factor C displaces DNA polymerase alpha prior to PCNA loading. J. Mol. Biol. 295: 791–801. https://doi.org/10.1006/jmbi.1999.3394

Maga, G., G. Villani, V. Tillement, M. Stucki, G. A. Locatelli et al., 2001 Okazaki fragment processing: modulation of the strand displacement activity of DNA polymerase delta by the concerted action of replication protein A, proliferating cell nuclear antigen, and flap endonuclease-1. Proc. Natl. Acad. Sci. USA 98: 14298–14303. https://doi.org/10.1073/pnas.251193198

Maringele, L., and D. Lydall, 2002 EXO1-dependent single-stranded DNA at telomeres activates subsets of DNA damage and spindle checkpoint pathways in budding yeast yku70Delta mutants. Genes Dev. 16: 1919–1933. https://doi.org/10.1101/gad.225102

Masuda-Sasa, T., P. Polaczek, X. P. Peng, L. Chen, and J. L. Campbell, 2008 Processing of G4 DNA by Dna2 helicase/nuclease and replication protein A (RPA) provides insights into the mechanism of Dna2/RPA substrate recognition. J. Biol. Chem. 283: 24359–24373. https://doi.org/10.1074/jbc.M802244200

Mimitou, E. P., and L. S. Symington, 2008 Sae2, Exo1 and Sgs1 collaborate in DNA double-strand break processing. Nature 455: 770–774. https://doi.org/10.1038/nature07312

Myler, L. R., I. F. Gallardo, Y. Zhou, F. Gong, S. H. Yang et al., 2016 Single-molecule imaging reveals the mechanism of Exo1 regulation by single-stranded DNA binding proteins. Proc. Natl. Acad. Sci. USA 113: E1170–E1179. https://doi.org/10.1073/pnas.1516674113

Navadgi-Patil, V. M., and P. M. Burgers, 2009a A tale of two tails: activation of DNA damage checkpoint kinase Mec1/ATR by the 9–1–1 clamp and by Dpb11/TopBP1. DNA Repair (Amst.) 8: 996–1003. https://doi.org/10.1016/j.dnarep.2009.03.011

Navadgi-Patil, V. M., and P. M. Burgers, 2009b The unstructured C-terminal tail of the 9-1-1 clamp subunit Ddc1 activates Mec1/ATR via two distinct mechanisms. Mol. Cell 36: 743–753. https://doi.org/10.1016/j.molcel.2009.10.014

Ngo, G. H., and D. Lydall, 2015 The 9–1–1 checkpoint clamp coordinates resection at DNA double strand breaks. Nucleic Acids Res. 43: 5017–5032. https://doi.org/10.1093/nar/gkv409

Ngo, G. H., L. Balakrishnan, M. Dubarry, J. L. Campbell, and D. Lydall, 2014 The 9–1-1 checkpoint clamp stimulates DNA resection by Dna2-Sgs1 and Exo1. Nucleic Acids Res. 42: 10516–10528. https://doi.org/10.1093/nar/gku746

Nugent, C. I., T. R. Hughes, N. F. Lue, and V. Lundblad, 1996 Cdc13p: a single-strand telomeric DNA-binding protein with a dual role in yeast telomere maintenance. Science 274: 249–252. https://doi.org/10.1126/science.274.5285.249

Ormö, M., A. B. Cubitt, K. Kallio, L. A. Gross, R. Y. Tsien et al., 1996 Crystal structure of the Aequorea victoria green fluorescent protein. Science 273: 1392–1395. https://doi.org/10.1126/science.273.5280.1392

Paeschke, K., M. L. Bochman, P. D. Garcia, P. Cejka, K. L. Friedman et al., 2013 Pif1 family helicases suppress genome instability at G-quadruplex motifs. Nature 497: 458–462. https://doi.org/10.1038/nature12149

Parenteau, J., and R. J. Wellinger, 1999 Accumulation of single-stranded DNA and destabilization of telomeric repeats in yeast mutant strains carrying a deletion of RAD27. Mol. Cell. Biol. 19: 4143–4152. https://doi.org/10.1128/MCB.19.6.4143

Peng, G., H. Dai, W. Zhang, H. J. Hsieh, M. R. Pan et al., 2012 Human nuclease/helicase DNA2 alleviates replication stress by promoting DNA end resection. Cancer Res. 72: 2802–2813. https://doi.org/10.1158/0008-5472.CAN-11-3152

Phillips, J. A., A. Chan, K. Paeschke, and V. A. Zakian, 2015 The pif1 helicase, a negative regulator of telomerase, acts preferentially at long telomeres. PLoS Genet. 11: e1005186. https://doi.org/10.1371/journal.pgen.1005186

Pike, J. E., P. M. Burgers, J. L. Campbell, and R. A. Bambara, 2009 Pif1 helicase lengthens some Okazaki fragment flaps necessitating Dna2 nuclease/helicase action in the two-nuclease processing pathway. J. Biol. Chem. 284: 25170–25180. https://doi.org/10.1074/jbc.M109.023325

Podust, V. N., L. M. Podust, F. Muller, and U. Hubscher, 1995 DNA polymerase delta holoenzyme: action on single-stranded DNA and on double-stranded DNA in the presence of replicative DNA helicases. Biochemistry 34: 5003–5010. https://doi.org/10.1021/bi00015a011

Puddu, F., M. Granata, L. Di Nola, A. Balestrini, G. Piergiovanni et al., 2008 Phosphorylation of the budding yeast 9–1–1 complex is required for Dpb11 function in the full activation of the UV-induced DNA damage checkpoint. Mol. Cell. Biol. 28: 4782–4793. https://doi.org/10.1128/MCB.00330-08

Rossi, M. L., and R. A. Bambara, 2006 Reconstituted Okazaki fragment processing indicates two pathways of primer removal. J. Biol. Chem. 281: 26051–26061. https://doi.org/10.1074/jbc.M604805200

Schulz, V. P., and V. A. Zakian, 1994 The saccharomyces PIF1 DNA helicase inhibits telomere elongation and de novo telomere formation. Cell 76: 145–155. https://doi.org/10.1016/0092-8674(94)90179-1

Sherman, F., G. R. Fink, and J. B. Hicks, 1986 Methods in Yeast Genetics. Cold Spring Harbor Laboratory, Cold Spring Harbor, NY.

Shim, E. Y., W. H. Chung, M. L. Nicolette, Y. Zhang, M. Davis et al., 2010 Saccharomyces cerevisiae Mre11/Rad50/Xrs2 and Ku proteins regulate association of Exo1 and Dna2 with DNA breaks. EMBO J. 29: 3370–3380. https://doi.org/10.1038/emboj.2010.219

Silva, S., I. Gallina, N. Eckert-Boulet, and M. Lisby, 2012 Live cell microscopy of DNA damage response in Saccharomyces cerevisiae. Methods Mol. Biol. 920: 433–443. https://doi.org/10.1007/978-1-61779-998-3_30

Soudet, J., P. Jolivet, and M. T. Teixeira, 2014 Elucidation of the DNA end-replication problem in Saccharomyces cerevisiae. Mol. Cell 53: 954–964. https://doi.org/10.1016/j.molcel.2014.02.030

Stewart, J. A., A. S. Miller, J. L. Campbell, and R. A. Bambara, 2008 Dynamic removal of replication protein A by Dna2 facilitates primer cleavage during Okazaki fragment processing in Saccharomyces cerevisiae. J. Biol. Chem. 283: 31356–31365. https://doi.org/10.1074/jbc.M805965200

Stith, C. M., J. Sterling, M. A. Resnick, D. A. Gordenin, and P. M. Burgers, 2008 Flexibility of eukaryotic Okazaki fragment maturation through regulated strand displacement synthesis. J. Biol. Chem. 283: 34129–34140. https://doi.org/10.1074/jbc.M806668200

Strauss, C., M. Kornowski, A. Benvenisty, A. Shahar, H. Masury et al., 2014 The DNA2 nuclease/helicase is an estrogen-dependent gene mutated in breast and ovarian cancers. Oncotarget 5: 9396–9409. https://doi.org/10.18632/oncotarget.2414

Sugiyama, T., E. M. Zaitseva, and S. C. Kowalczykowski, 1997 A single-stranded DNA-binding protein is needed for efficient presynaptic complex formation by the Saccharomyces cerevisiae Rad51 protein. J. Biol. Chem. 272: 7940–7945. https://doi.org/10.1074/jbc.272.12.7940

Tomita, K., T. Kibe, H. Y. Kang, Y. S. Seo, M. Uritani et al., 2004 Fission yeast Dna2 is required for generation of the telomeric single-strand overhang. Mol. Cell. Biol. 24: 9557–9567. https://doi.org/10.1128/MCB.24.21.9557-9567.2004

Waga, S., and B. Stillman, 1998 The DNA replication fork in eukaryotic cells. Annu. Rev. Biochem. 67: 721–751. https://doi.org/10.1146/annurev.biochem.67.1.721

Weinert, T. A., G. L. Kiser, and L. H. Hartwell, 1994 Mitotic checkpoint genes in budding yeast and the dependence of mitosis on DNA replication and repair. Genes Dev. 8: 652–665. https://doi.org/10.1101/gad.8.6.652

Weitao, T., M. Budd, and J. L. Campbell, 2003 Evidence that yeast SGS1, DNA2, SRS2, and FOB1 interact to maintain rDNA

stability. Mutat. Res. 532: 157–172. https://doi.org/10.1016/j.mrfmmm.2003.08.015

Wellcome Sanger Institute. COSMIC, the Catalogue Of Somatic Mutations In Cancer Database. Available at: http://cancer.13 sanger.ac.uk/cosmic. Accessed: September 19, 2017.

Wellinger, R. J., and V. A. Zakian, 2012 Everything you ever wanted to know about Saccharomyces cerevisiae telomeres: beginning to end. Genetics 191: 1073–1105. https://doi.org/10.1534/genetics.111.137851

Wu, P., H. Takai, and T. De Lange, 2012 Telomeric 3′ overhangs derive from resection by Exo1 and Apollo and fill-in by POT1b-associated CST. Cell 150: 39–52. https://doi.org/10.1016/j.cell.2012.05.026

Zhu, Z., W. H. Chung, E. Y. Shim, S. E. Lee, and G. Ira, 2008 Sgs1 helicase and two nucleases Dna2 and Exo1 resect DNA double-strand break ends. Cell 134: 981–994. https://doi.org/10.1016/j.cell.2008.08.037

Zou, L., and S. J. Elledge, 2003 Sensing DNA damage through ATRIP recognition of RPA-ssDNA complexes. Science 300: 1542–1548. https://doi.org/10.1126/science.1083430

Communicating editor: D. Bishop